MNRAS **000**, 1–?? (2017) Preprint 7 May 2019 Compiled using MNRAS LATEX style file v3.0

On the energy flux inside the pulsar magnetosphere

M. M. Rashkovetskyi[1], V. S. Beskin[2,3]⋆, A. K. Galishnikova[3], E. M. Novoselov[3] and A. A. Philippov[4]†

[1] *The Raymond and Beverly Sackler School of Physics and Astronomy, Tel Aviv University, Tel Aviv, 69978, Israel*
[2] *P.N.Lebedev Physical Institute, Leninsky prosp., 53, Moscow, 119991, Russia*
[3] *Moscow Institute of Physics and Technology, Dolgoprudny, Institutsky per., 9, Moscow Region, 141700, Russia*
[4] *Center for Computational Astrophysics, Flatiron Institute, 162 Fifth Avenue, New York, NY 10010, USA*

Accepted 2018 ; Received 2018 ; in original form 2018 April 1

ABSTRACT

To clarify the mechanism of energy losses in the pulsar magnetosphere the angular distribution of the electromagnetic (Poynting) energy flux at small distances from the star surface is explored. Analyzing the results of recent numerical simulation we found that almost all the energy flux is concentrated within narrow open magnetic field line region. We show that for large enough inclination angle between magnetic and rotation axis such angular distribution of the energy losses can be related to the separatrix currents which circulate in the pulsar magnetosphere but do not outflow into pulsar wind.

Key words: stars: neutron – pulsars: general.

1 INTRODUCTION

Starting with fundamental paper by Pacini (1967) it became clear that electromagnetic stresses play the main role in evolution of radio pulsars. It is not surprising that vacuum magneto-dipole radiation was considered for a long time as a main mechanism of the pulsar braking (Ostriker & Gunn 1969; Manchester & Taylor 1977). But later it became clear that the magnetosphere is to be filled with dense plasma that efficiently screens the longitudinal electric field; $E_\parallel = 0$ (Sturrock 1971; Mestel 1973). Moreover, it was shown that for zero longitudinal electric currents circulating in the pulsar magnetosphere the energy losses $W_{\rm tot}$ vanish for any inclination angle χ between the angular velocity $\mathbf{\Omega}$ and magnetic moment $\mathbf{m}$ (Beskin et al. 1983). This effect was confirmed later by Mestel et al. (1999) to be a result of full screening of the magneto-dipole radiation by magnetospheric plasma. This implies that the pulsar braking results fully from impact of the Ampère torque $\mathbf{K}$, which is a consequence of longitudinal currents flowing in the pulsar magnetosphere.

Nevertheless, magneto-dipole losses are still often mentioned in connection with the mechanism of energy release of radio pulsars. Indeed, MHD numerical simulations of the magnetosphere of inclined rotator obtained first by Spitkovsky (2006) and later confirmed in many papers (Kalapotharakos & Contopoulos 2009; Pétri 2012; Kalapotharakos et al. 2012; Tchekhovskoy et al. 2013; Philippov et al. 2014; Tchekhovskoy et al. 2016) demonstrate the following dependence of total energy losses on the inclination angle χ

$$W_{\rm tot}^{\rm MHD} \approx \frac{1}{4}\,\frac{B_0^2\Omega^4R^6}{c^3}(k_1 + k_2\,\sin^2\chi), \qquad (1)$$

where $k_1 = 1.0 \pm 0.1$ and $k_2 = 1.1 \pm 0.1$. As we see, this expression has the term with the same dependence on the angle χ as for magneto-dipole losses, indicating that magneto-dipole contribution could still exist. Unfortunately, recent numerical simulations (Kalapotharakos et al. 2012; Tchekhovskoy et al. 2016) have not clarified this question.

Remember that well-known analytical solution for so-called "inclined split-monopole" (Bogovalov 1999)

$$B_r = B_{\rm L}\frac{R_{\rm L}^2}{r^2}\,{\rm Sign}(\Psi), \qquad (2)$$

$$B_\varphi = E_\theta = -B_{\rm L}\,\frac{\Omega R_{\rm L}^2}{cr}\,\sin\theta\,{\rm Sign}(\Psi), \qquad (3)$$

where

$$\Psi = \cos\theta\cos\chi - \sin\theta\sin\chi\cos\left(\varphi - \Omega t + \Omega r/c\right), \qquad (4)$$

does not contain magneto-dipole wave since the electromagnetic fields outside of the current sheet located at the surface $\Psi = 0$ do not depend on time. For this reason it was not surprising that according to this model the energy losses do not depend on the inclination angle χ. However, as was shown by Kalapotharakos et al. (2012); Tchekhovskoy et al. (2016), MHD numerical simulation for large enough inclination angles $\chi > 30^\circ$ demonstrates a noticeable time-dependent component in the pulsar wind.

⋆ Contact e-mail: beskin@lpi.ru
† Contact e-mail: sphilippov@flatironinstitute.org

In particular, for orthogonal rotator (when the current sheet is actually absent) the solution has the following asymptotic behaviour at large distances $r \gg R_{\rm L}$, where $R_{\rm L} = c/\Omega$ is the light cylinder radius (Tchekhovskoy et al. 2016; Beskin 2018)

$$B_r \approx B_0 \frac{R^2}{r^2} \sin\theta \cos\Phi(r,\varphi,t), \quad (5)$$

$$B_\varphi = E_\theta \approx -B_0 \frac{\Omega R^2}{cr} \sin^2\theta \cos\Phi(r,\varphi,t), \quad (6)$$

where

$$\Phi(r,\varphi,t) = \varphi - \Omega t + \Omega r/c. \quad (7)$$

As we see, this asymptotic solution has the same wave factor $\Phi(r,\varphi,t)$ as for point orthogonal magnetic dipole rotating in vacuum (Landau & Lifshitz 1971)

$$B_r^\perp = \frac{|\mathbf{m}|}{r^3} \sin\theta \,{\rm Re}\left(2 - 2i\frac{\Omega r}{c}\right) \exp\left[i\Phi(r,\varphi,t)\right], \quad (8)$$

$$B_\theta^\perp = \frac{|\mathbf{m}|}{r^3} \cos\theta \,{\rm Re}\left(-1 + i\frac{\Omega r}{c} + \frac{\Omega^2 r^2}{c^2}\right) \exp\left[i\Phi(r,\varphi,t)\right], \quad (9)$$

$$B_\varphi^\perp = \frac{|\mathbf{m}|}{r^3} \,{\rm Re}\left(-i - \frac{\Omega r}{c} + i\frac{\Omega^2 r^2}{c^2}\right) \exp\left[i\Phi(r,\varphi,t)\right]. \quad (10)$$

This implies that displacement current does play important role in the pulsar wind zone.

Thus, the question arises about the nature of the electromagnetic torque acting on the neutron star. To clarify this point in this paper we analyze the angular distribution of the energy flux inside the light cylinder $r < R_{\rm L}$. We show that electromagnetic energy flux corresponding to MHD solution (1) does not contain a magneto-dipole wave. Inside the light cylinder all the energy flux outflows through the open flux tube region, and not quasi-isotropically, as it should have been the case for magneto-dipole radiation. Possible explanations of the nature of such an angular energy flux distribution are also discussed.

2 CURRENT LOSSES

2.1 Braking torque

To clarify how the braking of a radio pulsar occurs, let us remember the braking mechanism of a uniformly magnetized highly conducting rotating spherical ball. We note first of all that the rotating ball can be affected only by electromagnetic stress. The general expression for electromagnetic force $\mathrm{d}\mathbf{F}$ looks like

$$\mathrm{d}\mathbf{F} = \rho_{\rm e}\mathbf{E}\,\mathrm{d}V + \frac{[\mathbf{j}\times\mathbf{B}]}{c}\,\mathrm{d}V + \sigma_{\rm e}\mathbf{E}\,\mathrm{d}s + \frac{[\mathbf{J}_{\rm S}\times\mathbf{B}]}{c}\,\mathrm{d}s, \quad (11)$$

where the first two terms correspond to the volume contribution and the second two to the surface ones. Accordingly, the energy losses can be written down as

$$W_{\rm tot} = -\mathbf{\Omega}\mathbf{K}, \quad (12)$$

where

$$\mathbf{K} = \oint \mathbf{r}\times\mathrm{d}\mathbf{F} \quad (13)$$

is the electromagnetic torque.

However, if only the corotation currents $\mathbf{j} = \rho_{\rm e}[\mathbf{\Omega}\times\mathbf{r}]$ are assumed to flow in the bulk[1], then the volume part of the force $\mathrm{d}\mathbf{F}$ (11) vanishes due to freezing-in condition

$$\mathbf{E}_{\rm in} + \left[\frac{[\mathbf{\Omega}\times\mathbf{r}]}{c}\times\mathbf{B}_{\rm in}\right] = 0. \quad (14)$$

Moreover, electric surface term $\sigma_{\rm e}\mathbf{E}$ plays no role as well. Indeed, rewriting relations (12)–(13) as

$$\mathbf{\Omega}\cdot[\mathbf{r}\times\mathrm{d}\mathbf{F}] = \sigma_{\rm e}\mathbf{E}\cdot[\mathbf{\Omega}\times\mathbf{r}]\mathrm{d}s, \quad (15)$$

we see that due freezing-in condition (14) this scalar product vanishes. As a result, the general expression for the braking torque acting on a rotating magnetized sphere is

$$\mathbf{K} = \oint \left[\mathbf{r}\times\frac{[\mathbf{J}_{\rm s}\times\mathbf{B}]}{c}\right]\mathrm{d}s. \quad (16)$$

Thus, one can conclude that all the energy losses are indeed determined by the surface current $\mathbf{J}_{\rm s}$.

In what follows it will be more convenient to express the torque $\mathbf{K}$ through the magnetic field $\mathbf{B}$ only. As

$$\mathbf{J}_{\rm s} = \frac{c}{4\pi}[\mathbf{B}\times\mathbf{n}], \quad (17)$$

we obtain (Landau & Lifshitz 1971)

$$\mathbf{K} = \frac{R}{4\pi}\oint [\mathbf{n}\times\mathbf{B}]\,(\mathbf{B}\cdot\mathbf{n})\,\mathrm{d}s. \quad (18)$$

Here the first bracket corresponds to the surface current $\mathbf{J}_{\rm s}$, and the second one to the magnetic field in Ampère force $\mathbf{F} = [\mathbf{J}_{\rm s}\times\mathbf{B}]/c$. Together with (12) it finally gives

$$W_{\rm tot} = -\frac{\Omega R^3}{4\pi}\oint B_n B_\varphi \sin\theta\,\mathrm{d}s. \quad (19)$$

Clearly, this expression for the energy losses can be obtained directly from the electromagnetic flux

$$W_{\rm tot} = \frac{c}{4\pi}\oint [\mathbf{E}\times\mathbf{B}]\mathrm{d}\mathbf{s} \quad (20)$$

with $\mathbf{E}$ from (14). Accordingly, for spherical body this torque can be obtained also from the electromagnetic stress T_{kl}: $K_i = -\oint \varepsilon_{ijk} r_j T_{kl}\mathrm{d}s_l$.

It is important that expression (18) is correct not only for a neutron star surrounded by a magnetosphere filled with plasma (where the condition (14) holds) but also for a sphere rotating in vacuum. Indeed, assuming that the coordinate φ and time t entering all expressions only in the combination $\varphi - \Omega t$, the solution of Maxwell equation corresponding to Faraday law is well known to admit the form (see, e.g. Beskin 2010)

$$\mathbf{E} + \left[\frac{[\mathbf{\Omega}\times\mathbf{r}]}{c}\times\mathbf{B}\right] = -\nabla\psi. \quad (21)$$

On the other hand, according to freezing-in condition (14) one can conclude that $\psi = \mathrm{const}$ inside the sphere. Hence, at $r = R + 0$, the additional term $\nabla\psi$ is normal to the sphere surface. For this reason the contribution of $\nabla\psi$ to the electromagnetic energy flux (20) vanishes.

[1] Otherwise, in a rotating reference frame there would be an electric current in the absence of an electric field.

2.2 Magnetized sphere rotating in vacuum

To clarify some details of the braking mechanism responsible for MHD spin-down energy losses, let us consider at first uniformly magnetized sphere rotating in vacuum. Surprisingly, but even in this long-settled question there is one nontrivial point. Indeed, the total energy losses

$$W_{\rm tot} = \frac{2}{3}\,\frac{\mathbf{m}^2\Omega^4}{c^3}\,\sin^2\chi \tag{22}$$

depend only on the magnetic moment of the pulsar $\mathbf{m}$. However, the appropriate surface currents depend strongly on the fine structure of the magnetic field on the surface of the star.

To show this, we note that according to (12) and (22) the braking torque $\mathbf{K}$ (18) must be proportional to the third power of the angular velocity Ω. In other words, it must correspond to the third power of the expansion with respect to the small parameter

$$\varepsilon = \frac{\Omega R}{c}. \tag{23}$$

Further, one can show that the first order term $B^{(1)}$ turns out to be zero (see, e.g., Beskin & Zheltoukhov 2014 for more detail). In particular, it can be directly checked expanding the expressions (8)–(10) in terms of the small parameter ε. As a result, the general expression for the energy losses can be written as

$$W_{\rm tot} = -\frac{\Omega R^3}{4\pi}\oint\left(B_n^{(0)}B_\varphi^{(3)} + B_n^{(3)}B_\varphi^{(0)}\right)\sin\theta\,{\rm d}o, \tag{24}$$

where the indices (0) and (3) correspond to the expansion powers in parameter ε.

Recall now that classical Deutsch (1955) solution was constructed under the assumption that the normal component of the magnetic field exactly coincides with the field of the magnetic dipole. In particular, for orthogonal case the leading terms at the star surfce $r = R$ look like (Michel & Li 1999)

$$B_n = 2\,\frac{|\mathbf{m}|}{R^3}\,\sin\theta\,\cos\varphi, \tag{25}$$

$$B_\varphi = \frac{|\mathbf{m}|}{R^3}\,\left[\sin\varphi + \frac{1}{2}\varepsilon^2(\cos 2\theta - 2)\sin\varphi + \varepsilon^3\cos\varphi\right]. \tag{26}$$

In other words, by construction $B_n^{(3)} = 0$, so that the only contribution to the expression (24) for the braking torque is given by the first term.

On the other hand, expanding expressions (8)–(10) on the small value ε

$$B_n = \frac{|\mathbf{m}|}{R^3}\,\left[2\sin\theta\cos\varphi + \varepsilon^2\sin\theta\cos\varphi - \frac{2}{3}\varepsilon^3\sin\theta\sin\varphi\right], \tag{27}$$

$$B_\varphi = \frac{|\mathbf{m}|}{R^3}\,\left[\sin\varphi - \frac{1}{2}\varepsilon^2\sin\varphi - \frac{2}{3}\varepsilon^3\cos\varphi\right], \tag{28}$$

we find that only 2/3 of the losses are still determined by the first term in (24), while 1/3 with the second one. Certainly, the total energy losses and the direction of the evolution of the inclination angle χ do not depend on the choice of the solution.

This discrepancy can be easily explained. 'Point dipole' solution differs from the Deutsch solution by adding an additional magnetic dipole $\delta\mathbf{m}/|\mathbf{m}| = (\varepsilon^3/3)\mathbf{e}_y$, which generates homogeneous magnetic field inside the star

$$\mathbf{B}^{(3)} = -\frac{2}{3}\,\frac{|\mathbf{m}|}{R^3}\left(\frac{\Omega R}{c}\right)^3\mathbf{e}_{y'}, \tag{29}$$

where $\mathbf{e}_{y'}$ is the unit vector perpendicular to $\mathbf{\Omega}$ and $\mathbf{m}$. It is clear that appropriate electromagnetic losses are much less than even the electric quadrupole losses associated with the inevitable redistribution of charges inside the sphere. However, the structure of the surface currents changes radically.

Note that braking torque (18) does not depend on whether the zeroth-ordering currents are concentrated on the surface of the star or at its center. This is due to the fact that, similar to the additional magnetic field (29), the braking torque $\mathbf{K}$ does not depend on the radius of the sphere R for a fixed magnetic dipole $\mathbf{m}$.

2.3 Direct action of longitudinal magnetospheric current

Returning now to the problem of pulsar braking, remember that for zero longitudinal electric currents circulating in the pulsar magnetosphere the energy losses $W_{\rm tot}$ vanish for any inclination angle χ due to full screening of the magnetodipole radiation by magnetospheric plasma (Beskin et al. 1983; Mestel et al. 1999). This implies that the pulsar braking results fully from impact of the Ampère torque $\mathbf{K}$, which is a consequence of longitudinal currents flowing in the magnetosphere.

An example considering in the previous subsection helps us to understand the mechanism of such screening. It results from the disturbance of the third order components of the magnetic field $\mathbf{B}^{(3)}$ on the star surface. Clearly, it was impossible to determine all these components analytically. For this reason up to now only direct action of longitudinal magnetospheric current was included into consideration. In other words, only the first term in the expansion (24) (zero order $B_n^{(0)}$, third order $B_\varphi^{(3)}$ due to surface current which close longitudinal magnetospehric currents) was analyzed.

To determine the direct action of longitudinal magnetospheric currents $j_\parallel$ it is necessary to connect them by continuity equation

$$\nabla_2\mathbf{J}_{\rm s} = j_\parallel \tag{30}$$

with the surface current $\mathbf{J}_{\rm s}$. It is convenient to introduce dimensionless current $i = j_\parallel/j_{\rm GJ}$, where $j_{\rm GJ}$ is a 'local' Goldreich-Julian current density,

$$j_{\rm GJ} = -\frac{\Omega B\cos\theta_b}{2\pi}, \tag{31}$$

and θ_b is the angle between $\mathbf{\Omega}$ and $\mathbf{B}$. For dipole magnetic field near magnetic pole (and for $\varepsilon \ll 1$)

$$\theta_b \approx \chi - \frac{3}{2}\,\frac{r_m\cos\varphi_m}{R}, \tag{32}$$

where (r_m, φ_m) are the polar coordinates on the star surface relative to magnetic pole.

It is also convenient to split dimensionless current i into symmetric and anti-symmetric contributions, $i_{\rm s}$ and $i_{\rm a}$, depending upon whether the direction of the current is the same in the northern and southern parts of the polar cap,

or opposite. Using now the definition (32), we obtain for dipole magnetic field (and for $\varepsilon \ll 1$)

$$j_{\parallel,s}(r_m,\varphi_m) = -i_{\rm s}(r_m,\varphi_m)\frac{\Omega B}{2\pi}\cos\chi, \quad (33)$$

$$j_{\parallel,a}(r_m,\varphi_m) = -\frac{3}{2}\,i_{\rm a}(r_m,\varphi_m)\,\frac{\Omega B}{2\pi}\,\frac{r_m\cos\varphi_m}{R}\,\sin\chi \quad (34)$$

For $i_{\rm s}=i_{\rm a}=1$ we return to $j_\parallel=\rho_{\rm GJ}c$.

On the other hand, as was shown by Beskin et al. (1993), surface current $\mathbf{J}_{\rm s}$ can be present as

$$\mathbf{J}_{\rm s}=\nabla\xi. \quad (35)$$

In this case, the continuity equation (30) looks like

$$\frac{\partial^2\xi}{\partial x_m^2}+\frac{1}{x_m}\frac{\partial\xi}{\partial x_m}+\frac{1}{x_m^2}\frac{\partial^2\xi}{\partial\varphi_m^2}= \frac{\Omega BR^2}{2\pi}\left(i_{\rm s}\cos\chi+\frac{3}{2}\,i_{\rm a}\,x_m\cos\varphi_m\,\sin\chi\right), \quad (36)$$

where $x_m=r_m/R\ll 1$. As to boundary condition, it can be found under the assumption that beyond the polar cap there are no surface currents associated with the volume longitudinal current flowing in the magnetosphere (Beskin & Nokhrina 2004). In other words, this boundary condition can be formulated as the vanishing of the tangential surface current at the polar cap boundary

$$\xi\,[x_0(\varphi_m),\varphi_m]=\text{const}, \quad (37)$$

where the function $x_0(\varphi_m)$ prescribes the form of the polar cap. If we do not make this assumption, the problem of deceleration of the neutron star becomes uncertain since it is not possible to determine the magnitude of the additional surface current circulating outside the polar cap.

Continuity equation (36) together with boundary condition (37) allows us to determine surface current $\mathbf{J}_{\rm s}=\nabla\xi$ and, hence, braking torque $\mathbf{K}_{\rm vol}$ (16) and appropriate energy losses $W_{\rm vol}=-\mathbf{\Omega K}$

$$W_{\rm vol}=-\Omega\,K_\parallel\cos\chi-\Omega\,K_\perp\sin\chi. \quad (38)$$

Here we expand the torque $\mathbf{K}$ into two components parallel and perpendicular to the magnetic dipole moment $\mathbf{m}$

$$\mathbf{K}=K_\parallel\,\mathbf{e}_m+K_\perp\,\mathbf{n}_1, \quad (39)$$

where the unit vector $\mathbf{n}_1$ locates in the plain $\mathbf{\Omega m}$.

As a result, we obtain (see Appendix A for more detail)

$$K_{\rm vol,\parallel} = -c_\parallel\frac{B_0^2\Omega^3R^6}{c^3}\cos\chi, \quad (40)$$

$$K_{\rm vol,\perp} = -c_\perp\frac{B_0^2\Omega^3R^6}{c^3}\left(\frac{\Omega R}{c}\right)\sin\chi. \quad (41)$$

Here $B_0=2|\mathbf{m}|/R^3$ is the magnetic field at the magnetic pole, and the coefficients $c_\parallel\sim i_{\rm s}$ and $c_\perp\sim i_{\rm a}$ depend on current distribution functions $i_{\rm s}(r_m,\varphi_m)$ and $i_{\rm a}(r_m,\varphi_m)$. Accordingly, energy losses resulting from volume longitudinal currents can be present as

$$W_{\rm vol}=\frac{B_0^2\Omega^4R^6}{c^3}\left[c_\parallel\cos^2\chi+c_\perp\left(\frac{\Omega R}{c}\right)\sin^2\chi\right]. \quad (42)$$

Clearly, the coefficients $c_\parallel$ and $c_\perp$ depend also on the shape of the polar cap. But both analytical (Beskin et al. 1993) and numerical (Bai & Spitkovsky 2010; Gralla et al. 2017) results demonstrate that the disturbances of the polar cap boundary do not exceed 20% (see Fig. 1). Here to find the shape of the open magnetic line region deep inside the light cylinder from the results of numerical simulation we determine the domain with nonzero longitudinal currents $j_\parallel$ (nonzero scalar function Λ, see Appendix A2 for more detail).

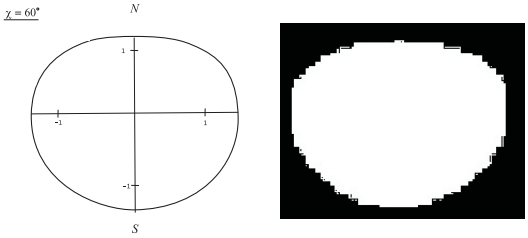

Figure 1. Polar cap shape for $\chi=60^\circ$ obtained analytically for the magnetosphere with zero longitudinal current $j_\parallel=0$ (Beskin et al. 1993, left) and using the results of numerical simulations produced by Tchekhovskoy et al. (2016) (right).

Finally, as was also stressed in Appendix A, the results of numerical simulations show that approximation $i_{\rm s}=\text{const}$, $i_{\rm a}=\text{const}$ is good enough to describe longitudinal currents flowing in the pulsar magnetosphere. It turned out that if the symmetric current is close to Goldreich-Julian one, the magnitude of the anti-symmetric current significantly exceeds it

$$i_{\rm s} \approx 1, \quad (43)$$

$$i_{\rm a} \approx \varepsilon^{-1/2}. \quad (44)$$

Thus, the assumptions about circular polar cap and constant dimensionless currents $i_{\rm s}$ and $i_{\rm s}$ are reasonable enough to restrict ourselves this model only.

As a result, for $i_{\rm a}=\text{const}$ and for circular polar cap the solution of continuity equation (36)

$$\xi(x_m,\varphi_m)=\frac{3i_{\rm a}}{32\pi}\,\Omega B_0R^2x_m(x_m^2-x_0^2)\,\sin\varphi_m \quad (45)$$

gives (Beskin et al. 1993)

$$c_\perp=\frac{f_*^3}{64}\,i_{\rm a}. \quad (46)$$

Certainly, were we took into account that the pulsar has two magnetic poles. Accordingly, for $i_{\rm s}=\text{const}$ we have

$$c_\parallel=\frac{f_*^2}{4}\,i_{\rm s}. \quad (47)$$

Here f_* is a dimensionless polar cap area:

$$s_{\rm cap}=f_*\pi R^2\left(\frac{\Omega R}{c}\right). \quad (48)$$

As was shown by Beskin et al. (1983) and confirmed recently by Tchekhovskoy et al. (2016) (see also Gralla et al. 2017),

$$f_*(\chi)\approx f_*(0)\,(1+0.2\,\sin^2\chi), \quad (49)$$

so that $f_*(\chi)$ increases from $f_*\approx 1.3$–1.5 for $\chi=0^\circ$ to $f_*\approx 1.7$–1.9 for $\chi=90^\circ$.

To summarize, we see that according to (42), (44) and (46), direct action of longitudinal electric currents for orthogonal rotator $W_{\rm vol}\sim\varepsilon^{1/2}W_{\rm tot}^{\rm MHD}$ is too small to explain total energy losses $W_{\rm tot}$. To satisfy MHD energy losses $W_{\rm tot}^{\rm MHD}$ (1) for $\chi=90^\circ$ the anti-symmetric current $i_{\rm a}$ should

be large enough: $i_a \approx \varepsilon^{-1}$. Thus, volume currents are too small to explain MHD energy losses, and we need to look for another possible contribution to the pulsar braking.

2.4 Additional torque: separatrix currents

At first, remember that, as was shown in Sect. 2.2, in addition to direct current losses mentioned above, the braking torque can be connected with the perturbation of the normal component of the magnetic field B_n. In this case, it is necessary to take into account the perturbation of the magnetic field over the entire surface of the neutron star, not only within polar cap. Such additional contribution could be related to the violation of the exact mutual compensation between the magneto-dipole radiation of the central star and the radiation of the magnetosphere itself taking place for zero longitudinal current.

On the other hand, there is another possible contribution to the pulsar braking. To discuss it let us return to energy losses due to surface current $\mathbf{J}_s$ closing magnetospheric longitudinal currents. Using the definition (16), it is convenient to rewrite now the total energy losses in the form

$$W_{\rm tot} = 2\,\frac{\Omega}{c}\int r_\perp J_\theta B_n {\rm d}s. \qquad (50)$$

Remember that analyzing expression (50) into the forehead, one can arrive at the erroneous conclusion that for local GJ current ($i_s = i_a = 1$), the braking torque should not strongly depend on the inclination angle χ. Indeed, as the angle χ increases, the surface current $\mathbf{J}_s$ decrease as $\cos\chi$. But the characteristic distance from the axis to the polar cap $r_\perp$, on the contrary, increases as $\sin\chi$.

However, as an accurate analysis shows (see again Appendix A1), this, at first glance, obvious reasoning does not take into account the real structure of the surface currents within polar cap region (Beskin et al. 1993). As shown in Figure 2, surface current should in fact be arranged in such a way that the current $< J_\theta >$ averaged over the polar cap surface (it is this component, as one can see from (50), determines the energy losses of the neutron star) would be zero. Therefore, in order to determine the energy losses, it was necessary to take into account effects of a higher order in the parameter $\varepsilon = \Omega R/c$.

By the way, if the averaged surface current $< J_\theta >$ is indeed zero, then, as shown in Figure 2, the surface current, which flows along the separatrix at the boundary of the closed magnetosphere, should be comparable to the total current flowing within the open field region region. For example, for a circular polar cap and local GJ current the return current is 75% of the volume current (see Appendix B1 and Beskin 2010 for more detail):

$$\frac{I_{\rm sep}}{I_{\rm vol}} = \frac{3}{4}. \qquad (51)$$

Here, however, one very important remark should be made. As was already stressed, the above conclusion that $< J_\theta >= 0$ was based on the assumption that there are no longitudinal currents in the closed magnetosphere (Beskin & Nokhrina 2004). The same concerns the separatrix currents that do not propagate in the pulsar wind. If we do not make these assumptions, the problem of deceleration of the neutron star becomes uncertain, since it is not possible to calculate the magnitude of the additional current circulating in the magnetosphere, but not outgoing into the pulsar wind region. Indeed, as shown in Figure 2, additional separatrix currents must inevitably lead to a nonzero average surface current $< J_\theta > \neq 0$ on the polar cap, and, consequently, to additional energy losses.

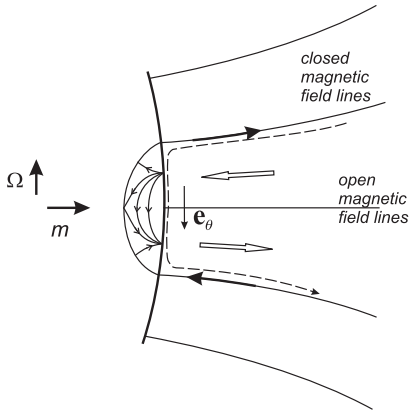

Figure 2. The structure of the volume (contour arrows), separatrix (fat arrows) and surface (thin arrows) currents near the polar cap of the orthogonal rotator. The additional separatrix current is shown by a dashed curve. Surface current $\mathbf{J}_s = \nabla\xi$ corresponds to solution $\xi(x_m, \varphi_m)$ (45).

Thus, it was not possible to achieve definitive clarity in the analytical analysis here. Some clarification became possible only after the results of numerical modeling for the magnetosphere of the inclined rotator were obtained. As a result, it was shown that volume currents in the closed magnetosphere are really absent. A remarkable event was also the fact that return currents along the separatrix were also confirmed (Bai & Spitkovsky 2010). However, the return current was found to be only 20% of the volume current. This discrepancy could be explained by the fact that in the calculations carried out, the star radius R was only two to three times smaller the light cylinder radius $R_{\rm L} = c/\Omega$. However, a significant difference in these quantities could also be associated with additional separatrix currents that were not taken into account in the previous analysis.

3 RESULTS

Returning now to the discussion of the energy losses of a neutron star, we recall that current losses connected with torque $K_{{\rm vol},\perp}$ (41) correspond to the first term in the expansion (24). They are caused by surface currents that close the volume currents flowing in the magnetosphere. Therefore, the action of such a braking torque is concentrated only in the area of the polar cap. The magnetic field here corresponds to the magnetic field of the zeroth approximation. In this case, as we have seen, volume current losses can not explain the energy release of $W_{\rm tot}^{\rm MHD}$ (1) for the MHD solution.

On the other hand, as was shown above, there are two more possible causes of the deceleration of radio pulsars. First, the example of vacuum losses shows that in general case the second term in the expansion (24) can be important. In this case, in the expression $\mathbf{J}_s \times \mathbf{B}$, the surface current

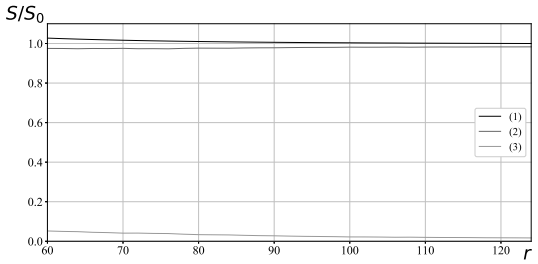

Figure 3. Electromagnetic energy flux from the region of closed (lower curve) and open (middle curve) magnetic field lines. The upper curve corresponds to the total energy losses. The radius of the neutron star (50 cells) is 10 times smaller than the radius of the light cylinder.

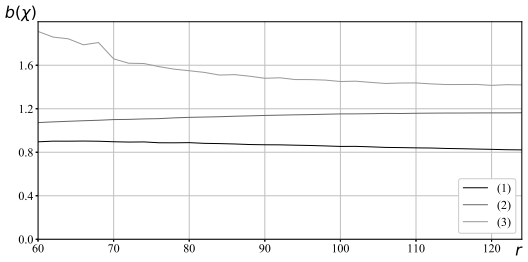

Figure 4. Dimensionless averaged radiative magnetic field $b(\chi)$ (56) for inclination angles $\chi = 30°$ (lower curve), 60° (middle), and 90° (upper curve) for $\varepsilon = 0.1$.

$\mathbf{J}_s$ corresponds to the zero-order current, and the magnetic field is related to the third-order perturbation induced by the rotation. Another possible cause may be associated with additional separatrix currents closing within the polar cap when energy losses still correspond to the first term in the expansion (24). Up to now these currents could not be predicted analytically, but we can use the results of numerical simulations to distinguish them.

Indeed, there is clear difference between two possibilities mentioned above. Energy losses connected with the second term in the expansion (24) are to be homogeneously distributed over the star surface. Consequently, in this case it can be expected that appropriate energy flux within the light cylinder is also distributed rather uniformly. On the other hand, energy losses connected with additional separatrix current are to be concentrated within the polar cap, i.e., appropriate energy flux is to be concentrated within open magnetic field line region. Thus, one can distinguish these two possibilities by analyzing the angular distribution of energy losses deep inside the light cylinder.

In Figure 3 we show the dependence of the electromagnetic energy flux S (determined from numerical results obtained by Tchekhovskoy et al. 2016) on the radius r for the inclination angle 60° through the region of closed (lower curve) and open (middle curve) field lines. As was already stressed, to find the area of the open magnetic field lines inside the light cylinder we determine numerically the region with nonzero longitudinal currents $j_\parallel$. The upper curve corresponds to the total energy losses. The flux S_0 corresponds to energy losses $W_{\rm tot}^{\rm MHD}$ (1). The size of the star is 50 cells, and the light cylinder is 500 cells ($\varepsilon = 0.1$).

As we see, practically all the energy flux is concentrated within open magnetic field region. There is no energy flux from the closed region which should have occurred if the second term in (24) was important. Hence, one can suppose that the most part of energy losses of the inclined rotator are associated with additional separatrix currents. We can also conclude that the above result does not leave any room for magneto-dipole losses. Remember that according to (25)–(26) and (27)–(28) the energy flux of vacuum magneto-dipole radiation near the star surface should be distributed quasi-homogeneously, $S(\theta) \propto \sin^2\theta$, and would not be concentrated within polar caps.

Using now relation (50), one can obtain an expression for the surface current averaged over the polar cap (here r_m and φ_m are again polar cap coordinates)

$$< J_\theta >= \frac{1}{s_{\rm cap}} \int J_\theta \, r_m {\rm d}r_m {\rm d}\varphi_m, \qquad (52)$$

that provides the main part of MHD energy losses $W_{\rm tot}^{\rm MHD}$ (1) for the orthogonal rotator

$$< J_\theta >= \frac{(k_1+k_2)}{2} \frac{c}{4\pi f_*} B_0 \left(\frac{\Omega R}{c}\right)^2. \qquad (53)$$

Here we neglect the direct action of volume currents. Accordingly, the averaged toroidal magnetic field $< B_\varphi >$ within open field lines region at the distance r is to be equal to

$$< B_\varphi >= \frac{(k_1+k_2)}{2} \frac{1}{f_*} B_0 \left(\frac{\Omega R}{c}\right)^2 \frac{R}{r}. \qquad (54)$$

It can be directly obtained by determining the energy flux through the corresponding area $s(r) = f_* \pi (\Omega/c)\, r^3$. For arbitrary inclination angle χ the appropriate component of the magnetic field (which is perpendicular to the plane containing $\mathbf{\Omega}$ and $\mathbf{m}$) is

$$B_\perp = B_\varphi \cos\varphi + B_\theta \sin\varphi. \qquad (55)$$

In Fig. 4 we show the dimensionless averaged radiative magnetic field $b(\chi)$ determined as (see Appendix C for more detail)

$$< B_\varphi >= b(\chi) \frac{1}{f_*} B_0 \left(\frac{\Omega R}{c}\right)^2 \frac{R}{r} \qquad (56)$$

for three different inclination angles $\chi = 30°$, 60°, and 90°, also taken from MHD numerical simulations obtained by Gralla et al. (2017) ($\varepsilon = 0.1$). As we see, for large enough distances from the the star (but certainly within the light cylinder) the r-dependence of $< B_\varphi >$ indeed corresponds to (54). Thus, radiative magnetic field $B_\perp$ behaves in the same way as in a magneto-dipole wave, but at small, not large distances $r \ll R_{\rm L}$.

Moreover, in Table 1 we present comparison of numerical (see Fig. 4) and analytical (relation C2) evaluations of dimensionless radiative magnetic field $b(\chi)$ (56). The uncertainties are mainly due to inaccuracy in the quantities f_*, k_1 and k_2. As we see, here we have good enough agreement as well.

As a result, it becomes clear why there was a difference between separatrix current $I_{\rm sep}$ found by Bai & Spitkovsky (2010) ($I_{\rm sep}$ is about 20% of the volume current) and the predicted value 75% (51). For a circular polar cap and homogeneous surface current distribution, separatrix current can be

Table 1. Comparison of numerical (see Fig. 4) and analytical (C2) evaluations of dimensionless radiative magnetic field $b(\chi)$ (56).

χ	30°	60°	90°
$b(\chi)$ (numerical)	0.8	1.2	1.4
$b(\chi)$ (analytical)	0.6 ± 0.1	1.0 ± 0.1	1.2 ± 0.1

determined analytically, and we obtain (see Appendix B2)

$$\frac{I_{\rm sep}}{I_{\rm vol}} = \frac{3}{4} - \frac{2}{f_*^{3/2}} \left(\frac{\Omega R}{c}\right)^{1/2}. \qquad (57)$$

It gives $I_{\rm sep} \sim$ (0.2–0.3) $I_{\rm vol}$, which is in good agreement with the result obtained by Bai & Spitkovsky (2010) (they have $\Omega R/c = 0.3$).

It is necessary to stress that for ordinary radio pulsars ($P \sim 1$ s, i.e. $(\Omega R/c)^{1/2} \sim 10^{-2}$) additional separatrix current $I_{\rm sep}^{\rm add}$ is 100 times smaller than the volume current $I_{\rm vol}$ circulating in the magnetosphere of orthogonal rotator. This property can be easily understood. Indeed, due to our normalization procedure $i_{\rm A} \sim (\Omega r/c)^{-1/2}$ (A16) volume current circulating in the magnetosphere of orthogonal rotator

$$I_{\rm vol} = \frac{i_{\rm a}}{2\pi} \frac{\Omega B_0}{R} R_0^3 \qquad (58)$$

just corresponds to volume current circulating in the magnetosphere of aligned rotator. But the distance from the axis $r_\perp$ in (16) for orthogonal rotator is $(\Omega r/c)^{-1/2}$ times larger that for axisymmetric case. For this reason much smaller additional separatrix current is enough to make a significant contribution to the energy losses.

Remember that so far we discuss the properties of MHD solution predicting energy losses $W_{tot}^{\rm MHD}$ (1). But let us write down now the additional braking torque in general form as

$$K_\perp^{\rm add} = -A \frac{B_0^2 \Omega^3 R^6}{c^3} i_{\rm a}, \qquad (59)$$

and try to estimate the dimensionless constant A from the results of numerical modeling. Since, as was shown, in this case the dimensionless longitudinal current is estimated as $i_{\rm a} \sim (\Omega R/c)^{-1/2}$, then the coefficient A turns out to be equal to

$$A \sim (\Omega R/c)^{1/2}. \qquad (60)$$

For such a small value $A \ll 1$, one can neglect the magnetospheric contribution $K_\perp^{\rm add}$ (59) for the local GJ current $i_{\rm a} \sim 1$ for $\chi \neq 90°$, which was done within the framework of BGI model (Beskin et al. 1993).

4 CONCLUSION

Thus, direct analysis of the angular distribution of the energy flux inside the light cylinder demonstrates that the energy flux is concentrated within narrow region of open magnetic field lines. At first, this implies the absence of magneto-dipole losses which angular distribution is to be more homogeneous. As to pulsar wind, it should be considered as an example of a relativistic magneto-hydrodynamical wave, which unusual properties (e.g., important role of displacement current) were previously unknown. For example, the angular distribution of the energy flux in the pulsar wind varies from $\sin^2\theta$ for axisymmetric case to $\sin^4\theta$ for the orthogonal rotator. Already in this point there is a significant difference from magneto-dipole losses, for which the losses at large distances are proportional to $(1+\cos^2\theta)$ (Landau & Lifshitz 1971). The absence of energy flux along the axis of rotation (i.e., at $\theta = 0$) for the inclination angle $\chi = 60°$ was already noted by Beskin et al. (2013) by the direct analysis of the results of numerical simulation performed by Spitkovsky (2006).

Further, we have shown the importance of additional separatrix currents circulating in the pulsar magnetosphere which provide the most energy losses for incline rotator. It is important that these currents connect both magnetic poles of a rotating neutron star, but do not outflow beyond the light cylinder. For electromagnetic waves in vacuum this is a common case (electric currents of the point dipole are located well inside the light cylinder), as the energy is transported by electromagnetic (Pointing) flux. The same takes place in relativistic MHD wave under consideration.. The amplitude of this current is to be much smaller than the total current circulating in the magnetosphere. For this reason the structure of this current near the light cylinder is unclear. Numerical simulations give us only the qualitative indication of its existence; quantitative consideration was not produced yet.

Finally, we would like to draw attention to the following circumstance. Starting from Shitov (1983), the additional bending of magnetic field lines $\delta\varphi_{\rm rot} = 1.2(r/R_{\rm L})^3 \sin^2\chi$ was widely considered in the analysis of mean profiles of radio pulsars (see, e.g., Lyne & Graham-Smith 2006). But this value was obtained for magneto-dipole mechanism of pulsar braking when the disturbance of toroidal magnetic field (29) is small enough. As was demonstrated above, radiative toroidal magnetic field (54) is much larger. Accordingly, much larger is to be the bending angle

$$\delta\varphi_{\rm rot} \approx \left(\frac{r}{R_{\rm L}}\right)^2 \sin^2\chi. \qquad (61)$$

Direct detection of such a large bending angle should be independent confirmation of large enough longitudinal current $j_\parallel \sim \varepsilon^{-1/2} j_{\rm GJ}$ predicted by MHD numerical simulation.

5 ACKNOWLEDGEMENTS

We thank Ya.N. Istomin for his interest and useful discussions. This work was partially supported by the government of the Russian Federation (agreement No. 05.Y09.21.0018) and by Russian Foundation for Basic Research (Grant no. 17-02-00788).

REFERENCES

Bai X.-N., Spitkovsky A., 2010, ApJ, 715, 1282
Beskin V. S., 2010, MHD flows in Compact Astrophysical Objects. Springer, Berlin
Beskin V., 2018, Phys. Uspekhi, 61
Beskin V. S., Nokhrina E. E., 2004, Astron. Lett., 30, 685
Beskin V. S., Zheltoukhov A. A., 2014, Phys. Uspekhi, 57, 799
Beskin V. S., Gurevich A. V., Istomin I. N., 1983, Sov. Phys. JETP, 58, 235

Beskin V., Gurevich A., Istomin Y., 1993, Physics of the Pulsar Magnetosphere. Cambridge University Press, Cambridge
Beskin V. S., Istomin Y. N., Philippov A. A., 2013, Phys. Uspekhi, 56, 164
Bogovalov S. V., 1999, A&A, 349, 1017
Deutsch A., 1955, Ann. d'Astrophys., 18, 1
Gralla S., Lupsasca A., Philippov A., 2017, ApJ, 851, 137
Kalapotharakos C., Contopoulos I., 2009, A&A, 496, 495
Kalapotharakos C., Contopoulos I., Kazanas D., 2012, MNRAS, 420, 2793
Landau L. D., Lifshitz E. M., 1971, The Classical Theory of Fields.. Pergamon Press, Oxford
Lyne A., Graham-Smith F., 2006, Pulsar astronomy. Cambridge University Press, Cambridge
Manchester R. N., Taylor J. H., 1977, Pulsars. W. H. Freeman, San Francisco
Mestel L., 1973, Astrophys. Space Sci., 24, 289
Mestel L., Panagi P., Shibata S., 1999, MNRAS, 309, 388
Michel F., Li H., 1999, Phys. Rep., 318, 227
Ostriker J. P., Gunn J. E., 1969, Nature, 221, 454
Pacini F., 1967, Nature, 216, 567
Pétri J., 2012, MNRAS, 424, 605
Philippov A., Tchekhovskoy A., Li J. G., 2014, MNRAS, 441, 1879
Shitov Y. P., 1983, Sov. Astron., 27, 314
Spitkovsky A., 2006, ApJ, 648, L51
Sturrock P., 1971, ApJ, 164, 529
Tchekhovskoy A., Spitkovsky A., Li J. G., 2013, MNRAS, 435, L1
Tchekhovskoy A., Philippov A., Spitkovsky A., 2016, MNRAS, 457, 3384

This paper has been typeset from a TEX/LATEX file prepared by the author.

APPENDIX A: BRAKING TORQUE BY SYMMETRIC AND ANTI-SYMMETRIC CURRENTS

A1 Basic equations

In this Appendix we remember the general explressions for braking torque due to surface current $\mathbf{J}_\mathrm{s}$ closing longitudinal magnetospheric currents $j_\parallel$ (Beskin et al. 1993). Using definitions (16) and (35), we obtain for two components of the braking torque $\mathbf{K} = K_\parallel\,\mathbf{e}_m + K_\perp\,\mathbf{n}_1$ (39):

$$K_\parallel = -\frac{B_0^2 R^4 \Omega}{c}\int_0^{2\pi}\frac{\mathrm{d}\varphi_m}{2\pi}\int_0^{x_0(\varphi_m)}\mathrm{d}x_m\,x_m^2\sqrt{1-x_m^2}\,\frac{\partial\xi}{\partial x_m}, \tag{A1}$$

and $K_\perp = K_1 + K_2$, where

$$K_1 = \frac{B_0^2 R^4 \Omega}{c}\int_0^{2\pi}\frac{\mathrm{d}\varphi_m}{2\pi}\int_0^{x_0(\varphi_m)}\mathrm{d}x_m A(x_m,\varphi_m), \tag{A2}$$

$$K_2 = \frac{B_0^2 R^4 \Omega}{c}\int_0^{2\pi}\frac{\mathrm{d}\varphi_m}{2\pi}\int_0^{x_0(\varphi_m)}\mathrm{d}x_m\,x_m^3\cos\varphi_m\,\frac{\partial\xi}{\partial x_m} \tag{A3}$$

and

$$A(x_m,\varphi_m) = x_m\cos\varphi_m\frac{\partial\xi}{\partial x_m} - \sin\varphi_m\frac{\partial\xi}{\partial\varphi_m}. \tag{A4}$$

Here again $x_m = r_m/R$, and we also took into account that both magnetic poles contribute to the slowing-down moment.

Since integration over x_m in (A2)–(A3) is taken to the polar cap boundary $x_0(\varphi_m) \sim \varepsilon^{1/2}$, as an estimate, we could take $K_2 \sim \varepsilon K_1$, i.e., $K_2 \ll K_1$. However, as is readily checked, when the boundary condition (37) is satisfied, the integrand in (A2) is a complete derivative with respect to φ_m:

$$\int_0^{x_0(\varphi_m)}\mathrm{d}x_m\left(x_m\cos\varphi_m\frac{\partial\xi}{\partial x_m} - \sin\varphi_m\frac{\partial\xi}{\partial\varphi_m}\right) = \frac{\partial}{\partial\varphi_m}\left[-\int_0^{x_0(\varphi_m)}\mathrm{d}x_m\,\xi\sin\varphi_m + \xi\left(x_0,\varphi_m\right)x_0(\varphi_m)\sin\varphi_m\right]. \tag{A5}$$

Therefore, the contribution K_1 appears identically equal to zero.

A2 Current structure

Here we show that the precision of approximation $i_\mathrm{s} = \mathrm{const}$ and $i_\mathrm{a} = \mathrm{const}$ is good enough to describe longitudinal currents flowing in the pulsar magnetosphere. At first, remember that the key role in particle motion in the pulsar magnetosphere belongs to the electric drift associated with a strong electric field produced by the rotation of a neutron star. As a result, the electric current component transverse to magnetic field $j_\perp$ can be written in the hydrodynamical form $\mathbf{j}_\perp = \rho_\mathrm{e}\mathbf{U}_\mathrm{dr}$, where

$$\mathbf{U}_\mathrm{dr} = c\frac{[\mathbf{E}\times\mathbf{B}]}{B^2} \tag{A6}$$

is the electric drift velocity.

Using now freezing-in condition (14), we obtain

$$\mathbf{j} = \rho_\mathrm{e}[\mathbf{\Omega}\times\mathbf{r}] + \Lambda\mathbf{B}, \tag{A7}$$

where Λ is a scalar function. The convenience of presentation (A7) connects with the fact that scalar function Λ must be constant along magnetic field lines. Indeed, using another Maxwell equation $\nabla\times\mathbf{B} = \ldots$ written under the assumption of quasi-stationarity (Mestel 1973; Beskin et al. 1983)

$$\nabla\times\left(\mathbf{B} - [\frac{[\mathbf{\Omega}\times\mathbf{r}]}{c}\times\mathbf{E}]\right) = \frac{4\pi}{c}(\mathbf{j} - \rho_\mathrm{e}[\mathbf{\Omega}\times\mathbf{r}]), \tag{A8}$$

we immediately obtain that $\mathbf{B}\cdot\nabla\Lambda = 0$.

According to (A7), near the star surface where $B_r \gg B_\varphi$, longitudinal current $j_\parallel$ can be present as $j_\parallel = \Lambda B_0$. In particular, as was recently shown by Gralla et al. (2017), parameter Λ corresponding to numerical MHD solution $W_\mathrm{tot} \propto 1+\sin^2\chi$ (1) can be extrapolated as[2]

$$\Lambda = -\frac{\Omega}{2\pi}\left[J_0(\tau)\cos\chi + J_1(\tau)\cos\varphi_m\cos\chi\right], \tag{A9}$$

where

$$\tau = 2\,\arcsin(\varepsilon^{-1/2}f_*^{-1/2}x_m). \tag{A10}$$

Here again $\varepsilon = \Omega R/c$, f_* is dimensionless polar cap area, and $J_0(\tau)$ and $J_1(\tau)$ are Bessel functions of the first kind. Comparing this expression for $\tau \ll 1$

$$\Lambda = -\frac{\Omega}{2\pi}\left[\cos\chi + \varepsilon^{-1/2}f_*^{-1/2}x_m\cos\varphi_m\cos\chi\right] \tag{A11}$$

with our definition (33)–(34), we obtain

$$i_\mathrm{s} \approx 1, \tag{A12}$$

$$i_\mathrm{a} \approx \frac{2}{3}f_*^{-1/2}\varepsilon^{-1/2}. \tag{A13}$$

For orthogonal case the value i_a can be also evaluated from orthogonal wind solution (5)–(6). Indeed, using radial component of Maxwell equation

$$\frac{1}{r\sin\theta}\frac{\partial}{\partial\theta}(B_\varphi\sin\theta) = \frac{4\pi}{c}j_r = \frac{4\pi}{c}\Lambda B_r \tag{A14}$$

we immediately obtain

$$\Lambda = -\frac{3}{4\pi}\Omega\cos\theta. \tag{A15}$$

Comparing now the total electric current $I = \int i_\parallel B_r\mathrm{d}s$ with Λ

[2] Here it is necessary to stress that this result was obtained under the assumption that the polar cap is circular.

from (A15) flowing through the upper hemisphere of the orthogonal wind (5)–(6) and the total current flowing through the northern part of the polar cap on the surface of a star (and taking into account that the value Λ is constant along magnetic field lines), one can obtain (Beskin 2018)

$$i_{\rm a} \approx f_*^{-1/2}\,\varepsilon^{-1/2}. \tag{A16}$$

A3 Braking torque

As was mentioned above, both analytical (Beskin et al. 1983) and numerical (Bai & Spitkovsky 2010; Gralla et al. 2017) simulations demonstrate that the disturbances of the polar cap boundary do not exceed 20%. Analyzing now relations (A1), (A3) one can find that for circular polar cap region $x_0 = {\rm const}$ only φ-independent values $i_{\rm s}(r_m)$ and $i_{\rm a}(r_m)$ contribute to the braking torque components $K_\parallel$ and $K_\perp$ (the contribution of all other terms of the expansion in terms of a and bsin $n\varphi$ and $\cos n\varphi$ vanish).

As a result, the expressions for $K_\parallel$ and $K_\perp$ have the form

$$K_\parallel = -c_\parallel \frac{B_0^2\Omega^3R^6}{c^3}\cos\chi, \tag{A17}$$

$$K_\perp = -c_\perp \frac{B_0^2\Omega^3R^6}{c^3}\left(\frac{\Omega R}{c}\right)\sin\chi, \tag{A18}$$

where $c_\parallel \sim i_{\rm s}$ and $c_\perp \sim i_{\rm a}$ are given by expressions (46) and (47). In general case these factors dependent on the particular profile of the longitudinal current $i_{\rm s}(r_m,\varphi_m)$ and $i_{\rm a}(r_m,\varphi_m)$ and on the form of the polar cap.

APPENDIX B: SEPARATRIX CURRENTS

B1 Separatrix currents due to volume currents flowing within open magnetic fild lines

For simplicity, let us consider orthogonal rotator ($\chi = 90^\circ$) with a circular polar cap. We also suppose that the volume current flowing along open magnetic field lines is proportional to local Goldreich-Julian charge density (32), i.e. $j_\parallel = i_{\rm a} j_{\rm GJ}$, $i_{\rm a} = {\rm const}$, where now

$$j_{\rm GJ} = \frac{\mathbf{\Omega B}}{2\pi} = \frac{3}{2}\frac{\Omega B}{2\pi}\frac{r_m\sin\varphi_m}{R}. \tag{B1}$$

Then the total volume current $I_{\rm vol}$ inflowing in the north hemisphere and outflowing from the south one within one polar cap is

$$I_{\rm vol} = \int_0^{R_0}\int_0^{\pi} j_\parallel r_m {\rm d}r_m {\rm d}\varphi_m = \frac{i_{\rm a}}{2\pi}\frac{\Omega B_0}{R}R_0^3. \tag{B2}$$

Using now explicit expression for the surface current $\mathbf{J}_{\rm s} = \nabla\xi$, where the potential ξ is given by (45) and again supposing the absence of surface currents outside the polar cap ($\nabla\xi = 0$ for $r_m > R_0$), we can determine the surface separatrix current $J_{\rm sep}$ through the jump of radial derivative

$$J_{\rm sep}(\varphi_m) = \{\nabla_r\xi\} = \frac{3i_{\rm a}}{16\pi}\Omega B_0 R^2\frac{R_0^2}{R^3}\sin\varphi_m. \tag{B3}$$

Integrating this value along the polar cap boundary in the upper hemisphere, we finally obtain for total separatrix current

$$I_{\rm sep} = \int_0^{\pi} J_{\rm sep}(\varphi_m)R_0{\rm d}\varphi_m = \frac{3i_{\rm a}}{8\pi}\frac{\Omega B_0}{R}R_0^3, \tag{B4}$$

in agreement with (51).

B2 Additional separatrix current

Suppose now that along the separatrix there is additional electric current resulting in surface current $J_{\rm s}^{\rm add}$. Again for simplicity we assume that within polar cap this surface current is homogeneous: $\mathbf{J}_s^{\rm add} = J^{\rm add}\mathbf{e}_\theta$ ($J^{\rm add} = {\rm const}$), i.e. for $r_m < R_0$

$$J_r^{\rm add} = -J^{\rm add}\sin\varphi_m, \tag{B5}$$

$$J_\varphi^{\rm add} = -J^{\rm add}\cos\varphi_m. \tag{B6}$$

The main difference with the current structure considered above in Appendix B1, is that here the surface currents exist not only inside, but also outside the polar cap (just for this reason they were previously rejected). Indeed, solving continuity equation (36) with zero r.h.s. and with the boundary condition (37), we obtain for $x_m > x_0$

$$J_r^{\rm add} = J^{\rm add}\sin\varphi_m\left(\frac{x_0}{x_m}\right)^2, \tag{B7}$$

$$J_\varphi^{\rm add} = -J^{\rm add}\cos\varphi_m\left(\frac{x_0}{x_m}\right)^2. \tag{B8}$$

It gives for the separatrix current

$$J_{\rm sep}^{\rm add}(\varphi_m) = \{\nabla_r\xi\} = 2J^{\rm add}\sin\varphi_m. \tag{B9}$$

Thus, the total additional separatrix current is

$$I_{\rm sep}^{\rm add} = \int_0^{\pi} J_{\rm sep}(\varphi_m)R_0{\rm d}\varphi_m = 4R_0J^{\rm add}, \tag{B10}$$

one half closing inside the polar cape while the second half outside it.

On the other hand, to determine the magnitude of the additional separatrix currrent $I_{\rm sep}^{\rm add}$ one can use general expression (50). As a result, we immediately reproduce (53). Finally, gathering together expressions (A16), (B2), and (B10), we obtain

$$\frac{I_{\rm sep}^{\rm add}}{I_{\rm vol}} = -\frac{k_1+k_2}{f_*^{3/2}}\left(\frac{\Omega R}{c}\right)^{1/2}. \tag{B11}$$

For $k_1 = k_2 = 1$ we return to (60).

Here it is necessary to stress that surface currents outside the polar cap do not contribute to energy losses. This property connects with different sign in (B7) in comparison with (B5). For this reason energy losses outside the polar cap are proportional to $(\sin^2\varphi_m - \cos^2\varphi_m)$. Being integrated over φ_m, they vanish.

APPENDIX C: ADDITIONAL TOROIDAL MAGNETIC FIELD

In this Appendix we evaluate the expected value of average radiative magnetic field $< B_\varphi >$ which we define through the dimensionless parameter $b(\chi)$ (56). Accordingly, energy losses connected with additional separatrix electric current looks like (again do not forget that pulsar has two magnetic poles)

$$W_{\rm sep} = \frac{b(\chi)}{2}\frac{B_0^2\Omega^4R^6}{c^3}\sin\chi. \tag{C1}$$

As was already stressed, energy losses $W_{\rm vol}$ (42) are too small to explain MHD energy losses $W_{\rm tot}^{\rm MHD}$ (1). Nevertheless, for $\Omega R/c \sim 0.1$ these terms can make a significant contribution to the energy budget. For this reason the expective value for parameter $b(\chi)$ can be presented as

$$b(\chi) = \left[\frac{k_1+k_2}{2} - \frac{f_*^{5/2}}{32}\left(\frac{\Omega R}{c}\right)^{1/2}\right]\sin\chi. \tag{C2}$$

Remember that evaluations (54)–(56) correspond to our assumption that longitudinal volume electric current is proportional to local Goldreich-Julian current $j_{\rm GJ}$ (32). As was shown recently by Gralla et al. (2017), this assumption agrees with numerical simulation.